ЖЭТФ, 2016, том 149, вып. 6, стр. 1137–1148 © 2016

DYNAMICS FOR A TWO-ATOM TWO-MODE INTENSITY-DEPENDENT RAMAN COUPLED MODEL

S. Singh [*]***, K. Gilhare***

University Department of Physics, Ranchi University
834008, Ranchi, Jharkhand State, India

Received November 16, 2015

We study the quantum dynamics of a two-atom Raman coupled model interacting with a quantized bimodal field with intensity-dependent coupling terms in a lossless cavity. The unitary transformation method used to solve the time-dependent problem also gives the eigensolutions of the interaction Hamiltonian. We study the atomic-population dynamics and dynamics of the photon statistics in the two cavity modes, and present evidence of cooperative effects in the production of antibunching and anticorrelations between the modes. We also investigate the effect of detuning on the evolution of second-order correlation functions and observe that the oscillations become more rapid for large detuning.

DOI: 10.7868/S0044451016060043

1. INTRODUCTION

The Jaynes–Cummings model (JCM) [1] of a single two-level atom interacting with a single quantized field mode in the dipole and rotating wave approximation constitutes a foundation for multiple studies in quantum optics. The intensity-dependent JCM proposed by Buck and Sukumar takes the coupling between matter and radiation to depend on the intensity of the electromagnetic field [2, 3]. The model has been investigated extensively for a general functional dependence and also for different field inputs. It has been observed that this model presents absolutely periodic revivals [4], contrary to what happens in the ordinary JCM, and displays other quantum effects such as the squeezing effect and the phase characteristic of the field [5, 6]. It is well known that intensity-dependent effects must be taken into account in two-photon processes. Although various extensions of the JCM with intensity-dependent coupling have been studied for single-atom two-mode two-photon processes [7–12], few research have so far been reported on the quantum dynamics of many or two-atom nondegenerate processes with intensity-dependent coupling [13].

Since the work of Dicke [14], the problem of collective emission from a sample of identical two-level atoms have received much attention and it was shown that cooperative effects can enhance some nonclassical effects [15–17]. Cooperative behavior in the production of correlations in light beams has also been reported for the intensity-dependent two-mode quantized cavity fields in the ladder configuration [13]. It then seems worthwhile to investigate the possibility of cooperative behavior in the intensity-dependent two-mode Raman coupled model.

This paper describes the intensity-dependent coupling for atomic transitions involving emission and absorption of photons via a Raman-type process. This model is relevant since this kind of interaction means that the coupling is proportional to the amplitude of the field, which is a very simple case of a nonlinear interaction corresponding to a more realistic physical situation.The intensity-dependent coupling model reflects a physically realistic situation in plasmonics, where the field is enhanced many orders of magnitude by the plasmonic effect. Even at a low light level, nonlinearity can be achieved, and hence quantum nonlinear optics is becoming a hot topic.

In this paper, we study the quantum dynamics of the two-atom Raman coupled model interacting with two quantized cavity fields, generalizing the corresponding Hamiltonian in [8, 17–20] by introducing an intensity-dependent coupling term [2, 3, 9, 10, 21, 22].

For obtaining the eigenfunctions and eigenvalues of the Hamiltonian of the interacting system, a straightforward method, that of the unitary transformation

[*] E-mail: vasudha_rnc1@rediffmail.com, sudhhasingh@gmail.com

in quantum mechanics by Sudha Singh [22], has been used. The method is mathematically simpler and more general.

The paper is arranged as follows. In Sec. 2, we present the two-atom two-mode intensity-dependent Raman coupled model describing the Dicke-type [14] atomic states and obtain expressions for the eigenfunctions and eigenvalues of the Hamiltonian of the interacting system. The atomic dynamics of the two-atom system and its behavior for different values of two-photon detuning parameter are studied in Sec. 3. The time dependence of the mean number of photons in the mode is analyzed in Sec. 4. In Sec. 5, we calculate the second-order correlation functions and study the cooperative nonclassical effects. We conclude with a brief summary.

2. TWO-MODE RAMAN MODEL WITH INTENSITY-DEPENDENT COUPLING

The effective Hamiltonian for a two-level atom with a transition frequency ω_0 interacting with two radiation fields of frequencies ω_1 and ω_2 via a two-mode Raman-type process can be written in the rotating wave approximation (RWA) as [8, 10, 18–20, 23]

$$\hat{H} = \frac{1}{2}\,\hbar\omega_0\hat{\sigma}_3 + \hbar\omega_1\hat{a}_1^\dagger\hat{a}_1 + \hbar\omega_2\hat{a}_2^\dagger\hat{a}_2 + \\ + \hbar\hat{g}\left(\hat{\sigma}_+\hat{a}_2^\dagger\hat{a}_1 + \hat{\sigma}_-\hat{a}_1^\dagger\hat{a}_2\right). \quad (1)$$

Here, symbols $\hat{a}_j^\dagger$ and $\hat{a}_j$ $(j = 1, 2)$ represent the field creation and annihilation operators for modes 1 and 2. The atomic levels $|1\rangle$ and $|2\rangle$ have identical parities and do not admit dipole transitions between themselves. Each level is dipole-coupled to a different mode of the field with the set of intermediate states $|i\rangle$. If the interacting field modes are far from resonance with intermediate states, then the atom can be seen as an effective two-level atom by means of the adiabatic elimination of intermediate states. The pump radiation mode ω_1 and the Stokes radiation mode ω_2 are in a two-mode resonance with the transition $|1\rangle \to |2\rangle$ such that $\hbar\omega_0 = (E_2 - E_1) = \hbar(\omega_1 - \omega_2)$; g is the coupling strength and $\hat{\sigma}$ are the 2×2 Pauli matrices.

With Eq. (1), the intensity-dependent two-mode Raman model is obtained as [2, 3, 8–10, 21]

$$\hat{H} = \frac{\hbar\omega_0\hat{\sigma}_3}{2} + \hbar\omega_1\hat{a}_1^\dagger\hat{a}_1 + \hbar\omega_2\hat{a}_2^\dagger\hat{a}_2 + \\ + \hbar\hat{g}\left(\hat{\sigma}_+\sqrt{\hat{a}_2^\dagger\hat{a}_2}\,\hat{a}_2^\dagger\hat{a}_1\sqrt{\hat{a}_1^\dagger\hat{a}_1} + \right. \\ \left. + \hat{\sigma}_-\sqrt{\hat{a}_1^\dagger\hat{a}_1}\,\hat{a}_1^\dagger\hat{a}_2\sqrt{\hat{a}_2^\dagger\hat{a}_2}\right). \quad (2)$$

We construct the many-atom case as for the Dicke model [14].

The collective atomic operators $\hat{R}_1$, $\hat{R}_2$, and $\hat{R}_3$ are defined as

$$\hat{R}_l = \frac{1}{2}\sum_{j=1}^{N}\hat{\sigma}_l^j, \quad \hat{R}_\pm = \sum_{j=1}^{N}\hat{\sigma}_\pm^j, \quad (3)$$

where N is the number of atoms, $l = 1, 2, 3$, and $\hat{\sigma}_\pm^j$ are the atomic operators for the jth atom.

The operators $\hat{R}_\pm$, $\hat{R}_l$, and $\hat{R}^2 = \hat{R}_1^2 + \hat{R}_2^2 + \hat{R}_3^2$ obey the commutation relations for general angular momentum operators. The N-atom Hamiltonian is then obtained as

$$\hat{H} = \hbar\omega_0\hat{R}_3 + \hbar\omega_1\hat{a}_1^\dagger\hat{a}_1 + \hbar\omega_2\hat{a}_2^\dagger\hat{a}_2 + \hbar g\left(\hat{P}_+ + \hat{P}_-\right), \quad (4)$$

where

$$\hat{P}_+ = \hat{R}_+\sqrt{\hat{a}_2^\dagger\hat{a}_2}\,\hat{a}_2^\dagger\hat{a}_1\sqrt{\hat{a}_1^\dagger\hat{a}_1}, \\ \hat{P}_- = \hat{R}_-\sqrt{\hat{a}_1^\dagger\hat{a}_1}\,\hat{a}_1^\dagger\hat{a}_2\sqrt{\hat{a}_2^\dagger\hat{a}_2}. \quad (5)$$

We can write the basis vectors for the atomic system as $|\psi\rangle = |m_h\rangle$, where m_h represents the number of atoms in the higher-energy states. The different atom operators commute with one another and the following relations hold:

$$\hat{R}_3|m_h\rangle = (m_h - N/2)|m_h\rangle, \\ \hat{R}_+|m_h\rangle = (N - m_h)|m_h + 1\rangle, \\ \hat{R}_-|m_h\rangle = m_h|m_h - 1\rangle. \quad (6)$$

For the special case of two atoms, $N = 2$ and the possible two-atom states are

$$|0\rangle = |1\rangle_{A_1} \otimes |1\rangle_{A_2} = |1, 1\rangle_A, \\ |1\rangle = [|1\rangle_{A_1} \otimes |2\rangle_{A_2} + |2\rangle_{A_1} \otimes |1\rangle_{A_2}] = \\ = [|1, 2\rangle_A + |2, 1\rangle_A], \\ |2\rangle = |2\rangle_{A_1} \otimes |2\rangle_{A_2} = |2, 2\rangle_A, \quad (7)$$

where A_1 and A_2 represent atom 1 and atom 2. For the two-atom system, the Dicke states $|j, m\rangle_D$ have $j = 1$ with $m = 1, 0, -1$. These states are represented in terms of the two-atom states above as

$$|1, -1\rangle_D = |1, 1\rangle_A, \\ |1, 0\rangle_D = \frac{1}{\sqrt{2}}\,[|1, 2\rangle_A + |2, 1\rangle_A], \\ |1, 1\rangle_D = |2, 2\rangle_A. \quad (8)$$

The general state vector for the system at any time t can be written as

$$|\psi(t)\rangle = \sum_{n_1,n_2=0}^{\infty} \left[A_{1,1}^{n_1,n_2}(t)|0,n_1,n_2\rangle + A_{1,2}^{n_1,n_2}(t)|1,n_1-1,n_2+1\rangle + A_{2,2}^{n_1,n_2}(t)|2,n_1-2,n_2+2\rangle\right]. \quad (9)$$

In terms of the Dicke states in Eq. (8),

$$|\psi(t)\rangle = \sum_{n_1,n_2=0}^{\infty} \left[A_{-}^{n_1,n_2}(t)|1,-1\rangle_D|n_1,n_2\rangle_F + \sqrt{2}\,A_0^{n_1,n_2}(t)|1,0\rangle_D|n_1-1,n_2+1\rangle_F + A_{+}^{n_1,n_2}(t)|1,1\rangle_D|n_1-2,n_2+2\rangle_F\right]. \quad (10)$$

The state vector $|\psi(t)\rangle$ evolves unitarily from the state vector $|\psi(0)\rangle$ at $t=0$:

$$|\psi(t)\rangle = \hat{T}(t)|\psi(0)\rangle, \quad (11)$$

where the unitary operator $\hat{T}(t)$ satisfies the equation

$$i\hbar\frac{d\hat{T}(t)}{dt} = \hat{H}\hat{T}(t). \quad (12)$$

In the Heisenberg picture, $\hat{H}$ given by Eq. (4) becomes time independent under the condition $\omega_1-\omega_2 \approx \approx \omega_0$, and therefore Eq. (12) can be integrated with $\hat{H}$ given by (4) to obtain the unitary transformation operator

$$\hat{T} = \exp\left[-it\left\{\omega_0\hat{R}_3 + \omega_1\hat{a}_1^{\dagger}\hat{a}_1 + \omega_2\hat{a}_2^{\dagger}\hat{a}_2 + g\left(\hat{P}_+ + \hat{P}_-\right)\right\}\right]. \quad (13)$$

If we consider the initial state of the system to be $|0,n_1,n_2\rangle$, we obtain

$$|\psi(t)\rangle = \hat{T}(t)|0,n_1,n_2\rangle \quad (14)$$

from Eq. (11). To obtain the right-hand side of Eq. (14), we expand $\hat{T}(t)$ given by Eq. (13) and then act with each term of the expansion on $|0,n_1,n_2\rangle$ [7,8,22]. This yields the expression for the general state vector $|\psi(t)\rangle$ given in Appendix.

In the Heisenberg picture, the operators $\hat{P}_+$ and $\hat{P}_-$ become time-independent at the two-photon resonance. We use the following relations to obtain the general state vector $|\psi(t)\rangle$:

$$\begin{aligned}
&\hat{P}_+|0,n_1,n_2\rangle = 2n_1(n_2+1)|1,n_1-1,n_2+1\rangle,\\
&\hat{P}_+|1,n_1-1,n_2+1\rangle = (n_1-1)(n_2+2)\times\\
&\qquad\times|2,n_1-2,n_2+2\rangle,\\
&\hat{P}_-|1,n_1-1,n_2+1\rangle = n_1(n_2+1)|0,n_1,n_2\rangle,\\
&\hat{P}_-|2,n_1-2,n_2+2\rangle = 2(n_1-1)(n_2+2)\times\\
&\qquad\times|1,n_1-1,n_2+1\rangle,\\
&\hat{P}_-\hat{P}_+|0,n_1,n_2\rangle = 2n_1^2(n_2+1)^2|0,n_1,n_2\rangle,\\
&\hat{P}_-|0,n_1,n_2\rangle = \hat{P}_+|2,n_1-2,n_2+2\rangle = 0 \text{ etc.}
\end{aligned} \quad (15)$$

In view of Eq. (14) and Appendix, it follows that the respective coefficients of $|0,n_1,n_2\rangle$, $|1,n_1-1,n_2+1\rangle$, and $|2,n_1-2,n_2+2\rangle$ in Appendix give the probability amplitudes $A_{1,1}^{n_1,n_2}(t)$, $A_{1,2}^{n_1,n_2}(t)$, and $A_{2,2}^{n_1,n_2}(t)$.

The transition probability $|A_{+}^{n_1,n_2}(t)|^2$ is obtained from the coefficient of $|2,n_1-2,n_2+2\rangle$ in Appendix as

$$|A_{+}^{n_1,n_2}(t)|^2 = \frac{4g^4n_1^2(n_2+1)^2(n_1-1)^2(n_2+2)^2}{\Omega_{n_1,n_2}^4}\times \times\left(1-\cos\Omega_{n_1,n_2}t\right)^2, \quad (16)$$

where

$$\Omega_{n_1,n_2} = \sqrt{\Omega_R^2+\delta_{12}^2} \quad (17)$$

with

$$\Omega_R = g\sqrt{2\left\{n_1^2(n_2+1)^2+(n_1-1)^2(n_2+2)^2\right\}}, \quad (18)$$

and $\delta_{12} = \omega_0 - (\omega_1-\omega_2)$ is the two-photon detuning.

From the coefficient of $|1,n_1-1,n_2+1\rangle$ in Appendix, by algebraic simplifications, we obtain the expression for the transition probability

$$|A_0^{n_1,n_2}(t)|^2 = \frac{2g^2n_1^2(n_2+1)^2}{\Omega_R^2+\left(\dfrac{\delta_{12}}{2}\right)^2}\times \times\sin^2\left(\sqrt{\Omega_R^2+\left(\frac{\delta_{12}}{2}\right)^2}\right)t. \quad (19)$$

At the two-photon resonance, $\delta_{12}=0$, and hence

$$\Omega_{n_1,n_2} = \Omega_R = g\sqrt{2\left\{n_1^2(n_2+1)^2+(n_1-1)^2(n_2+2)^2\right\}}$$

and the above expression becomes

$$|A_0^{n_1,n_2}(t)|^2 = \frac{2g^2n_1^2(n_2+1)^2}{\Omega_R^2}\sin^2\Omega_Rt. \quad (20)$$

Similarly, the transition probability $|A_{-}^{n_1,n_2}(t)|^2$ is obtained from the coefficients of $|0,n_1,n_2\rangle$ in Appendix as

$$|A_{-}^{n_1,n_2}(t)|^2 = 1 - \frac{4g^2 n_1^2 (n_2+1)^2}{\Omega_{n_1,n_2}^2} \times \\ \times [1-\cos(\Omega_{n_1,n_2}t)] + \frac{4g^4 n_1^4 (n_2+1)^4}{\Omega_{n_1,n_2}^4} \times \\ \times \left[\frac{3}{2} - 2\cos(\Omega_{n_1,n_2}t) + \frac{1}{2}\cos(2\Omega_{n_1,n_2}t)\right]. \quad (21)$$

3. ATOMIC DYNAMICS

For the two field modes in an initial coherent state, the probability $W_{ee}(t)$ of finding both atoms in the excited state can be written as

$$W_{ee}(t) = \sum_{n_1=0}^{\infty}\sum_{n_2=0}^{\infty} P_{n_1}(\overline{n}_1)P_{n_2}(\overline{n}_2)|A_{+}^{n_1,n_2}(t)|^2, \\ W_{ee}(t) = \sum_{n_1=0}^{\infty}\sum_{n_2=0}^{\infty} P_{n_1}(\overline{n}_1)P_{n_2}(\overline{n}_2) \times \\ \times \frac{4g^4 n_1^2 (n_2+1)^2 (n_1-1)^2 (n_2+2)^2}{\Omega_{n_1,n_2}^4} \times \\ \times \left[\frac{3}{2} - 2\cos(\Omega_{n_1,n_2}t) + \frac{1}{2}\cos(2\Omega_{n_1,n_2}t)\right], \quad (22)$$

where

$$P_{n_i}(\overline{n}_i) = \exp(-\overline{n}_i)\frac{\overline{n}_i^{n_i}}{n_i!} \quad (i=1,2)$$

and $\overline{n}_i$ is the initial average number of photons in the ith mode; $P_{n_i}(\overline{n}_i)$ represent the coherent field probability distribution functions for photon numbers in the Poisson statistics.

The probability $W_{eg}(t)$ of finding one atom in the excited state and the other one in the ground state is obtained (at exact resonance) as

$$W_{eg}(t) = \frac{1}{2}\sum_{n_1=0}^{\infty}\sum_{n_2=0}^{\infty} P_{n_1}(\overline{n}_1)P_{n_2}(\overline{n}_2)|A_{0}^{n_1,n_2}(t)|^2 = \\ = \frac{1}{2}\sum_{n_1=0}^{\infty}\sum_{n_2=0}^{\infty} P_{n_1}(\overline{n}_1)P_{n_2}(\overline{n}_2)\frac{2g^2 n_1^2 (n_2+1)^2}{\Omega_R^2} \times \\ \times [1-\cos(2\Omega_R t)] \quad (23)$$

and the probability $W_{gg}(t)$ of finding both atoms in the ground state is given by

$$W_{gg}(t) = \sum_{n_1=0}^{\infty}\sum_{n_2=0}^{\infty} P_{n_1}(\overline{n}_1)P_{n_2}(\overline{n}_2)|A_{-}^{n_1,n_2}(t)|^2,$$

or

$$W_{gg}(t) = \sum_{n_1=0}^{\infty}\sum_{n_2=0}^{\infty} P_{n_1}(\overline{n}_1)P_{n_2}(\overline{n}_2) \times \\ \times \left[1 - \frac{4g^2 n_1^2 (n_2+1)^2}{\Omega_{n_1,n_2}^2}\{1-\cos(\Omega_{n_1,n_2}t)\} + \right. \\ \left. + \frac{4g^4 n_1^4 (n_2+1)^4}{\Omega_{n_1,n_2}^4}\left\{\frac{3}{2} - 2\cos(\Omega_{n_1,n_2}t) + \right.\right. \\ \left.\left. + \frac{1}{2}\cos(2\Omega_{n_1,n_2}t)\right\}\right]. \quad (24)$$

In the special case where the pump radiation mode is prepared initially in a coherent state, whereas the Stokes radiation mode is in a vacuum state ($\overline{n}_2 = 0$), we obtain

$$W_{ee}(t) = \sum_{n_1=0}^{\infty} P_{n_1}(\overline{n}_1)\frac{16g^4 n_1^2 (n_1-1)^2}{\Omega_{n_1,0}^4} \times \\ \times \left[\frac{3}{2} - 2\cos(\Omega_{n_1,0}t) + \frac{1}{2}\cos(2\Omega_{n_1,0}t)\right], \quad (25)$$

where

$$\Omega_{n_1,0} = \sqrt{\Omega_R'^2 + \delta_{12}^2},$$

$$W_{eg}(t) = \frac{1}{2}\sum_{n_1=0}^{\infty} P_{n_1}(\overline{n}_1)\frac{2g^2 n_1^2}{\Omega_R'^2 + \left(\frac{\delta_{12}}{2}\right)^2} \times \\ \times \left[1 - \cos\left(2\sqrt{\Omega_R'^2 + \left(\frac{\delta_{12}}{2}\right)^2}\right)t\right]. \quad (26)$$

At the two-photon resonance, $\delta_{12} = 0$, whence

$$\Omega_{n_1,0} = \Omega_R' = g\sqrt{2\{n_1^2 + 4(n_1-1)^2\}} = \\ = g\left[2(5n_1^2 - 8n_1 + 4)\right]^{1/2}. \quad (27)$$

Figures 1*a* and 1*b* display the time evolution of $W_{ee}(t)$ and $W_{eg}(t)$ with $\overline{n}_1 = 10$, $\overline{n}_2 = 0$ for $\delta_{12} = 0$ and $\delta_{12} = 20g$. Here, $\Omega_{n_1,0} = \sqrt{2}\,g(5\overline{n}_1^2 - 8\overline{n}_1 + 4)^{1/2} \approx \approx g\sqrt{10}(\overline{n} - 4/5)$ ($\overline{n} \gg 1$) becomes linear in the quantum number, and hence an exact periodic evolution is observed in Fig. 1. The two types of Rabi oscillations observed in the dynamics of W_{ee}, one at a smaller amplitude than the other, are due to respective one- and two-photon processes. Using the arguments in [13, 17], the collapse time t_c and the revival time t_R are obtained as

$$t_c = \frac{1}{2g\sqrt{10\overline{n}_1}}, \quad (28)$$

$$gt_R \approx \frac{2\pi}{\sqrt{10}}\,m, \quad m = 0, 1, 2, 3, \ldots \quad (29)$$

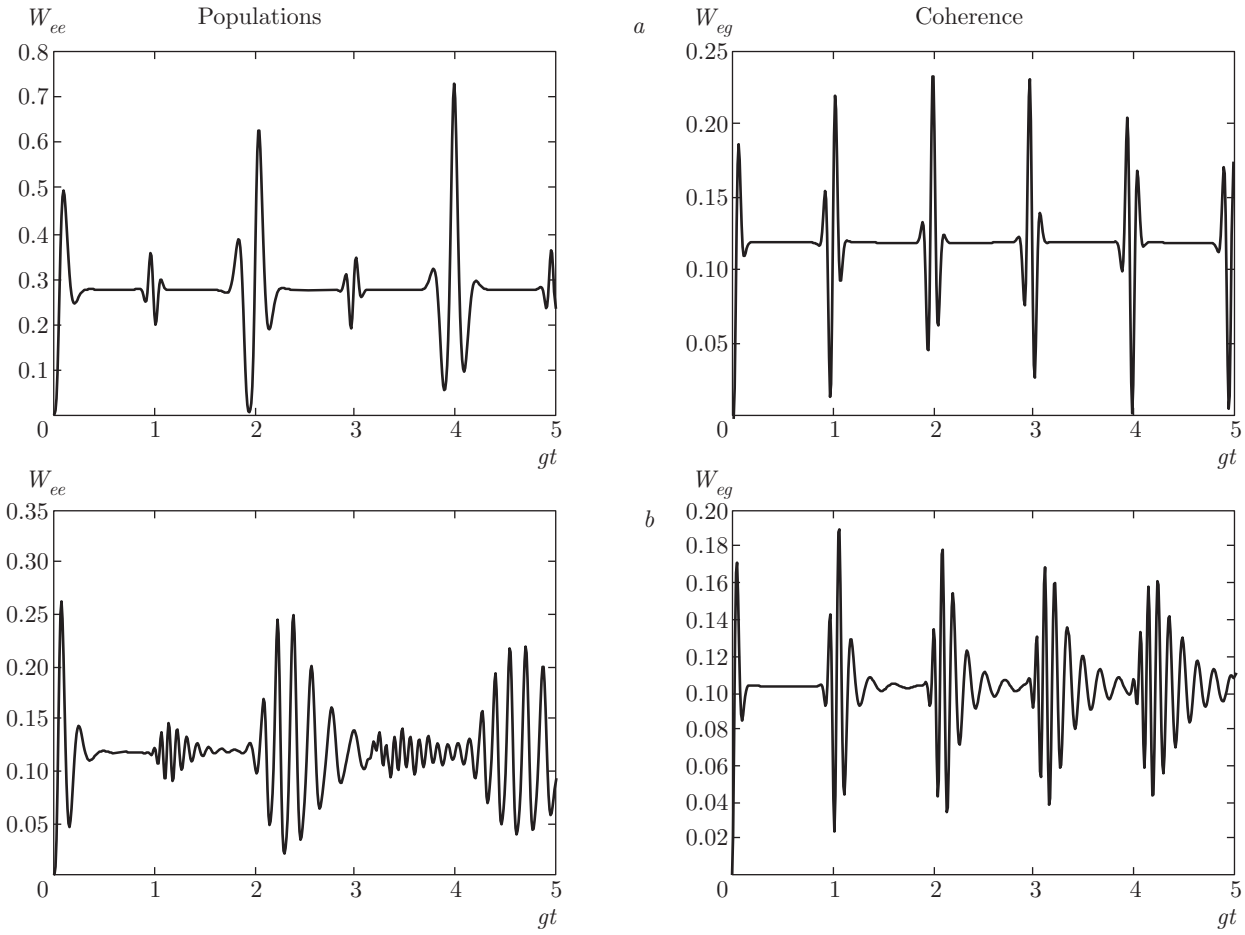

Fig. 1. Time evolutions of W_{ee} and W_{eg} for finite detunings: (a) $\delta_{12} = 0$, (b) $\delta_{12} = 20g$. Here, $\overline{n}_1 = 10$, $\overline{n}_2 = 0$

The revival time is independent of the mean number of photons. The ratio of the collapse time to the revival time is $t_c/t_R = 1/4\pi\overline{n}^{1/2}$, as in the usual JCM.

For $\overline{n}_1 = 10$ and $\overline{n}_2 = 0$, Eq. (29) predicts a large amplitude oscillations of W_{ee} at $gt_R = 1.99$, 3.97, etc., as observed in Fig. 1*a*. For the other terms in (25) that oscillate at the frequency $2\Omega_{n_1,0}$, we observe a smaller amplitude revival at $gt_R/2$. For W_{eg}, only the frequencies $2\Omega_{n_1,0}$ contribute and the revivals occur as expected at $gt_R = 0.99$, 1.99, 2.98, 3.98, etc.

It is observed that with the increase in detuning from zero to $\delta_{12} = 20g$, there is a decrease in the amplitude of Rabi oscillations and the oscillations become more rapid.

For $\overline{n}_1, \overline{n}_2 \neq 0$, the rapid oscillations are due to the dominant Rabi oscillations at

$$\Omega_{n_1,n_2} = g\sqrt{2\left\{\overline{n}_1^2(\overline{n}_2+1)^2 + (\overline{n}_1-1)^2(\overline{n}_2+2)^2\right\}}\,.$$

In this case, the Rabi frequency becomes proportional to the square of the quantum number n. As such, the exact periodicity that was observed in Fig. 1 for a single input photon is not observed in Fig. 2.

To obtain the revival time, we adopt the method used in [13,17]. For large $\overline{n}_1$ and $\overline{n}_2$, we obtain

$$gt_R = \frac{\pi\sqrt{kl}}{\sqrt{\overline{n}_1}\sqrt{\overline{n}_2}} = \frac{\pi\sqrt{m}}{\sqrt{\overline{n}_1}\sqrt{\overline{n}_2}}, \qquad kl = m = 0,1,2,\ldots \tag{30}$$

with the condition

$$\frac{\overline{n}_2}{\overline{n}_1} = \frac{k}{l}, \quad k = l = 0,1,2,3,\ldots \tag{31}$$

For a single-atom intensity-dependent two-mode Raman process [8], the Rabi frequency is $\Omega_{SA} = 2g\overline{n}_1 \times \times (\overline{n}_2 + 1)$, and we obtain an expression identical to Eq. (30):

$$(gt_R)_{SA} = \frac{\pi\sqrt{m}}{\sqrt{\overline{n}_1}\sqrt{\overline{n}_2}}, \quad m = 0,1,2,\ldots$$

For $\overline{n}_1 = \overline{n}_2 = 5$, Eq. (30) predicts the revivals at $gt_R = 0.62$, 0.88, 1.088, 1.25, 1.4, etc. as in case of

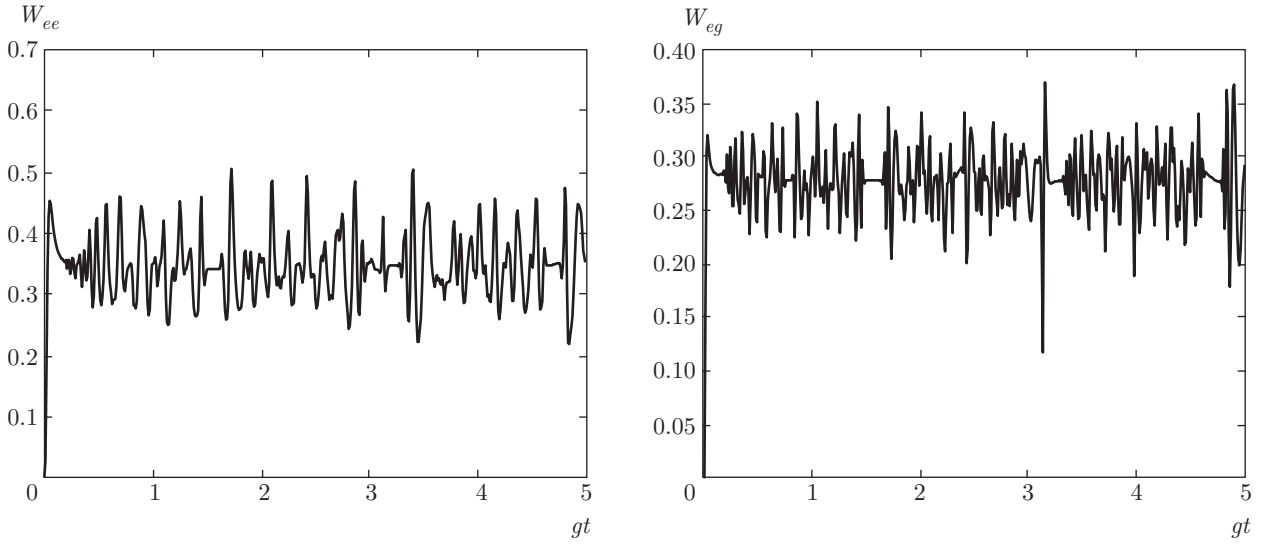

Fig. 2. Time evolutions of W_{ee} and W_{eg} for $\overline{n}_1 = 5$, and $\overline{n}_2 = 5$. Here $\delta_{12} = 0$

a single atom. Additional revivals present due to the terms oscillating at the frequency $2\Omega_{n_1,n_2}$ in Eq. (22) can be predicted to occur at

$$gt'_R = \frac{\pi\sqrt{m}}{2\sqrt{\overline{n}_1}\sqrt{\overline{n}_2}} = \frac{gt_R}{2}, \quad m = 0, 1, 2, \ldots \tag{32}$$

Equation (32) presents the revivals at $gt_R = 0.31$, 0.44, 0.54, 0.62, 0.7, etc. for $\overline{n}_1 = 5$ and $\overline{n}_2 = 5$. It is observed that although all the existing revivals obey analytic formula (30), a part of additional revivals predicted by Eq. (30) does not exist since Eq. (31) also has to be satisfied for values other than k and l used to generate the revival time.

4. MEAN NUMBER OF PHOTONS IN THE MODES

The mean number of photons in the modes can be calculated as

$$\begin{aligned}\langle a_1^\dagger(t)a_1(t)\rangle &= \\ &= \sum_{n_1=0}^{\infty}\sum_{n_2=0}^{\infty} n_1 P_{n_1}(\overline{n}_1)P_{n_2}(\overline{n}_2)|A_-^{n_1,n_2}(t)|^2 + \\ &+ 2\sum_{n_1=0}^{\infty}\sum_{n_2=0}^{\infty}(n_1-1)P_{n_1}(\overline{n}_1)P_{n_2}(\overline{n}_2)|A_0^{n_1,n_2}(t)|^2 + \\ &+ \sum_{n_1=0}^{\infty}\sum_{n_2=0}^{\infty}(n_1-2)P_{n_1}(\overline{n}_1)P_{n_2}(\overline{n}_2)|A_+^{n_1,n_2}(t)|^2, \end{aligned} \tag{33}$$

$$\begin{aligned}\langle a_2^\dagger(t)a_2(t)\rangle &= \\ &= \sum_{n_1=0}^{\infty}\sum_{n_2=0}^{\infty} n_2 P_{n_1}(\overline{n}_1)P_{n_2}(\overline{n}_2)|A_-^{n_1,n_2}(t)|^2 + \\ &+ 2\sum_{n_1=0}^{\infty}\sum_{n_2=0}^{\infty}(n_2+1)P_{n_1}(\overline{n}_1)P_{n_2}(\overline{n}_2)|A_0^{n_1,n_2}(t)|^2 + \\ &+ \sum_{n_1=0}^{\infty}\sum_{n_2=0}^{\infty}(n_2+2)P_{n_1}(\overline{n}_1)P_{n_2}(\overline{n}_2)|A_+^{n_1,n_2}(t)|^2. \end{aligned} \tag{34}$$

Figures 3*a* and 3*b* display the time evolution of the mean number of photons in mode 1 and mode 2 respectively for $\overline{n}_1 = 10$, $\overline{n}_2 = 0$ and $\overline{n}_1 = 5$, $\overline{n}_2 = 5$.

The structure of the collapses and revivals in Rabi oscillations for the mean number of photons is similar to the corresponding structure for atomic probabilities in Fig. 1*a* for $\overline{n}_1 = 10$ and $\overline{n}_2 = 0$ and in Fig. 2 for $\overline{n}_1 = 5$ and $\overline{n}_2 = 5$ because the time dependence of the mean number of photons is determined by the same harmonic time functions with the frequencies Ω_{n_1,n_2} and $2\Omega_{n_1,n_2}$.

5. FIELD STATISTICS

For investigating the nonclassical properties of the radiation field, we calculate the second-order correlation function [17, 19, 24]

$$G_{ij}^{(2)}(t) = \frac{\langle a_i^\dagger(t)a_j^\dagger(t)a_j(t)a_i(t)\rangle}{\langle a_i^\dagger(t)a_i(t)\rangle\langle a_j^\dagger(t)a_j(t)\rangle}, \quad i,j = 1,2. \tag{35}$$

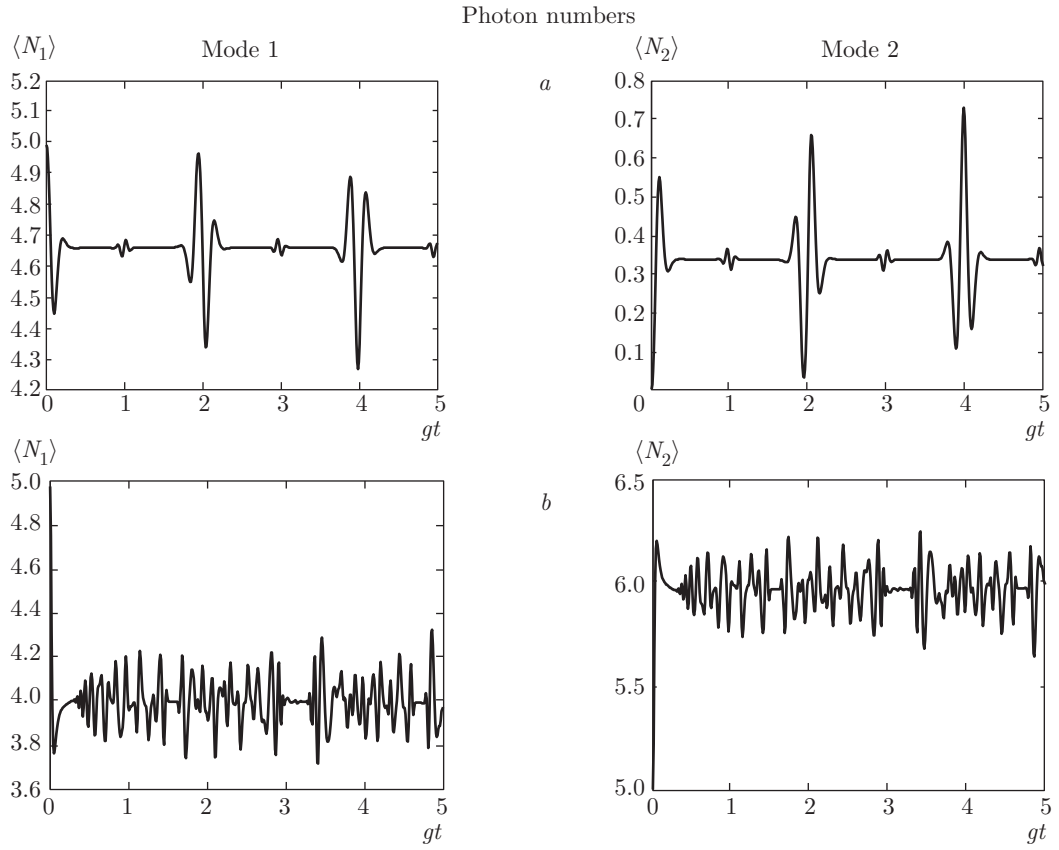

Fig. 3. Time evolutions of the photon numbers for modes 1 and 2 for (a) $\overline{n}_1 = 10$ and $\overline{n}_2 = 0$, (b) $\overline{n}_1 = 5$, $\overline{n}_2 = 5$

The second-order correlation function $G_{ii}^{(2)}$ is represented as

$$G_{ii}^{(2)}(t) = 1 + \frac{\langle : (\Delta N_i(t))^2 : \rangle}{\langle N_i(t)\rangle^2}, \quad i = 1, 2, \tag{36}$$

where $\langle N_i\rangle = \langle a_i^\dagger(t) a_i(t)\rangle$ is the mean number of photons and

$$\langle : (\Delta N_i(t))^2 : \rangle = \langle a_i^\dagger(t) a_i^\dagger(t) a_i(t) a_i(t)\rangle - \langle N_i(t)\rangle^2 \tag{37}$$

is the normally ordered uncertainty of the number of photons in the ith mode.

If $G_{ii}^{(2)} = 1$ or $\langle : (\Delta N_i(t))^2 : \rangle = 0$, the photons arrive at the detectors at random and the probability distribution is Poissonian. The bunching occurs when $G_{ii}^{(2)} > 1$ or $\langle : (\Delta N_i(t))^2 : \rangle > 0$ and the distribution is super-Poissonian. This is also a classical state (for example, $G_{ii}^{(2)} = 2$ or $\langle : (\Delta N_i(t))^2 : \rangle = 1$ for thermal light).

Whenever $G_{ii}^{(2)} < 1$ or $\langle : (\Delta N_i(t))^2 : \rangle < 0$, the light is nonclassical, exhibiting the sub-Poissionian statistics. Because we are calculating the zero time delay coherence function, the states satisfying these conditions are antibunched. The antibunched case is a quantum mechanical manifestation that has no counterpart in the classical description of radiation.

We obtain the following expressions for the quantities $\langle a_i^\dagger(t) a_i^\dagger(t) a_i(t) a_i(t)\rangle$ $(i = 1, 2)$ that are required for the numerical estimation of $\langle : (\Delta N_i(t))^2 : \rangle$:

$$\begin{aligned}
&\langle a_1^\dagger(t) a_1^\dagger(t) a_1(t) a_1(t)\rangle = \\
&= \sum_{n_1=0}^{\infty}\sum_{n_2=0}^{\infty} n_1(n_1-1) P_{n_1}(\overline{n}_1) P_{n_2}(\overline{n}_2) |A_-^{n_1,n_2}(t)|^2 + \\
&+ 2\sum_{n_1=0}^{\infty}\sum_{n_2=2}^{\infty} (n_1-1)(n_1-2) P_{n_1}(\overline{n}_1) P_{n_2}(\overline{n}_2) \times \\
&\times |A_0^{n_1,n_2}(t)|^2 + \\
&+ \sum_{n_1=0}^{\infty}\sum_{n_2=3}^{\infty} (n_1-2)(n_1-3) P_{n_1}(\overline{n}_1) P_{n_2}(\overline{n}_2) \times \\
&\times |A_+^{n_1,n_2}(t)|^2,
\end{aligned} \tag{38}$$

$$\langle a_2^\dagger(t)a_2^\dagger(t)a_2(t)a_2(t)\rangle =$$
$$= \sum_{n_1=0}^{\infty}\sum_{n_2=0}^{\infty} n_2(n_2-1)P_{n_1}(\overline{n}_1)P_{n_2}(\overline{n}_2)|A_-^{n_1,n_2}(t)|^2 +$$
$$+ 2\sum_{n_1=0}^{\infty}\sum_{n_2=0}^{\infty}(n_2+1)n_2P_{n_1}(\overline{n}_1)P_{n_2}(\overline{n}_2)\times$$
$$\times |A_0^{n_1,n_2}(t)|^2 +$$
$$+ \sum_{n_1=0}^{\infty}\sum_{n_2=0}^{\infty}(n_2+2)(n_2+1)P_{n_1}(\overline{n}_1)P_{n_2}(\overline{n}_2)\times$$
$$\times |A_+^{n_1,n_2}(t)|^2. \quad (39)$$

Using Eqs. (33) and (34) for $\langle a_i^\dagger(t)a_i(t)\rangle$ $(i=1,2)$, we numerically evaluate the quantities $\langle : (\Delta N_i(t))^2 : \rangle$.

For comparison, we refer to Eqs. (14) and (31) of our earlier paper [8] and write the expression for the general state vector for the atom initially in the lower state $|b\rangle$ and the field in the two-mode coherent state for the single-atom two-mode intensity-dependent Raman model as

$$|\psi(t)\rangle_{SA} =$$
$$= \sum_{n_1=0}^{\infty}\sum_{n_2=0}^{\infty} P_{n_1}(\overline{n}_1)P_{n_2}(\overline{n}_2)\left[b_{n_1,n_2}(t)|b,n_1,n_2\rangle + \right.$$
$$\left. + a_{n_1-1,n_2+1}(t)|a,n_1-1,n_2+1\rangle\right]. \quad (40)$$

We obtain the following expressions for a single-atom two-mode intensity-dependent process:

$$\langle a_1^\dagger(t)a_1(t)\rangle_{SA} =$$
$$= \sum_{n_1=0}^{\infty}\sum_{n_2=0}^{\infty} n_1P_{n_1}(\overline{n}_1)P_{n_2}(\overline{n}_2)|b_{n_1,n_2}|^2 +$$
$$+ \sum_{n_1=0}^{\infty}\sum_{n_2=0}^{\infty}(n_1-1)P_{n_1}(\overline{n}_1)P_{n_2}(\overline{n}_2)|a_{n_1-1,n_2+1}|^2, \quad (41)$$

$$\langle a_1^\dagger(t)a_1^\dagger(t)a_1(t)a_1(t)\rangle_{SA} =$$
$$= \sum_{n_1=0}^{\infty}\sum_{n_2=0}^{\infty} n_1(n_1-1)P_{n_1}(\overline{n}_1)P_{n_2}(\overline{n}_2)|b_{n_1,n_2}|^2 +$$
$$+ \sum_{n_1=0}^{\infty}\sum_{n_2=0}^{\infty}(n_1-1)(n_1-2)P_{n_1}(\overline{n}_1)P_{n_2}(\overline{n}_2)\times$$
$$\times |a_{n_1-1,n_2+1}|^2, \quad (42)$$

$$\langle a_2^\dagger(t)a_2(t)\rangle_{SA} =$$
$$= \sum_{n_1=0}^{\infty}\sum_{n_2=0}^{\infty} n_2P_{n_1}(\overline{n}_1)P_{n_2}(\overline{n}_2)|b_{n_1,n_2}|^2 +$$
$$+ \sum_{n_1=0}^{\infty}\sum_{n_2=0}^{\infty}(n_2+1)P_{n_1}(\overline{n}_1)P_{n_2}(\overline{n}_2)\times$$
$$\times |a_{n_1-1,n_2+1}|^2, \quad (43)$$

$$\langle a_2^\dagger(t)a_2^\dagger(t)a_2(t)a_2(t)\rangle_{SA} =$$
$$= \sum_{n_1=0}^{\infty}\sum_{n_2=0}^{\infty} n_2(n_2-1)P_{n_1}(\overline{n}_1)P_{n_2}(\overline{n}_2)|b_{n_1,n_2}|^2 +$$
$$+ \sum_{n_1=0}^{\infty}\sum_{n_2=0}^{\infty}(n_2+1)n_2P_{n_1}(\overline{n}_1)P_{n_2}(\overline{n}_2)\times$$
$$\times |a_{n_1-1,n_2+1}|^2. \quad (44)$$

Here,

$$|a_{n_1-1,n_2+1}|^2 = \sin^2\left[gtn_1(n_2+1)\right],$$
$$|b_{n_1,n_2}|^2 = 1-\sin^2\left[gtn_1(n_2+1)\right]. \quad (45)$$

The intermode second-order coherence is determined by

$$G_{12}^{(2)}(t) = \frac{\langle a_1^\dagger(t)a_2^\dagger(t)a_2(t)a_1(t)\rangle}{\langle a_1^\dagger(t)a_1(t)\rangle\langle a_2^\dagger(t)a_2(t)\rangle} =$$
$$= 1 + \frac{C(t)}{\langle a_1^\dagger(t)a_1(t)\rangle\langle a_2^\dagger(t)a_2(t)\rangle}, \quad (46)$$

where the cross-correlation function $C(t)$ defined as

$$C(t) = \langle a_1^\dagger(t)a_2^\dagger(t)a_2(t)a_1(t)\rangle -$$
$$- \langle a_1^\dagger(t)a_1(t)\rangle\langle a_2^\dagger(t)a_2(t)\rangle \quad (47)$$

represents the correlation between the intensities of the two modes of the field. If $C(t)>0$, then the two modes are correlated and if $C(t)=0$, the field modes are uncorrelated and independent. For $C(t)<0$, they are called anti-correlated. We obtain

$$\langle a_1^\dagger(t)a_2^\dagger(t)a_2(t)a_1(t)\rangle =$$
$$= \sum_{n_1=0}^{\infty}\sum_{n_2=0}^{\infty} n_1n_2P_{n_1}(\overline{n}_1)P_{n_2}(\overline{n}_2)|A_-^{n_1,n_2}(t)|^2 +$$
$$+ 2\sum_{n_1=0}^{\infty}\sum_{n_2=0}^{\infty}(n_1-1)(n_2+1)P_{n_1}(\overline{n}_1)P_{n_2}(\overline{n}_2)\times$$
$$\times |A_0^{n_1,n_2}(t)|^2 +$$
$$+ \sum_{n_1=0}^{\infty}\sum_{n_2=0}^{\infty}(n_1-2)(n_2+2)P_{n_1}(\overline{n}_1)P_{n_2}(\overline{n}_2)\times$$
$$\times |A_+^{n_1,n_2}(t)|^2. \quad (48)$$

At this point, we write the expression for $\langle a_1^\dagger(t)a_2^\dagger(t)a_2(t)a_1(t)\rangle$ for a single-atom two-mode Raman process with intensity-dependent coupling:

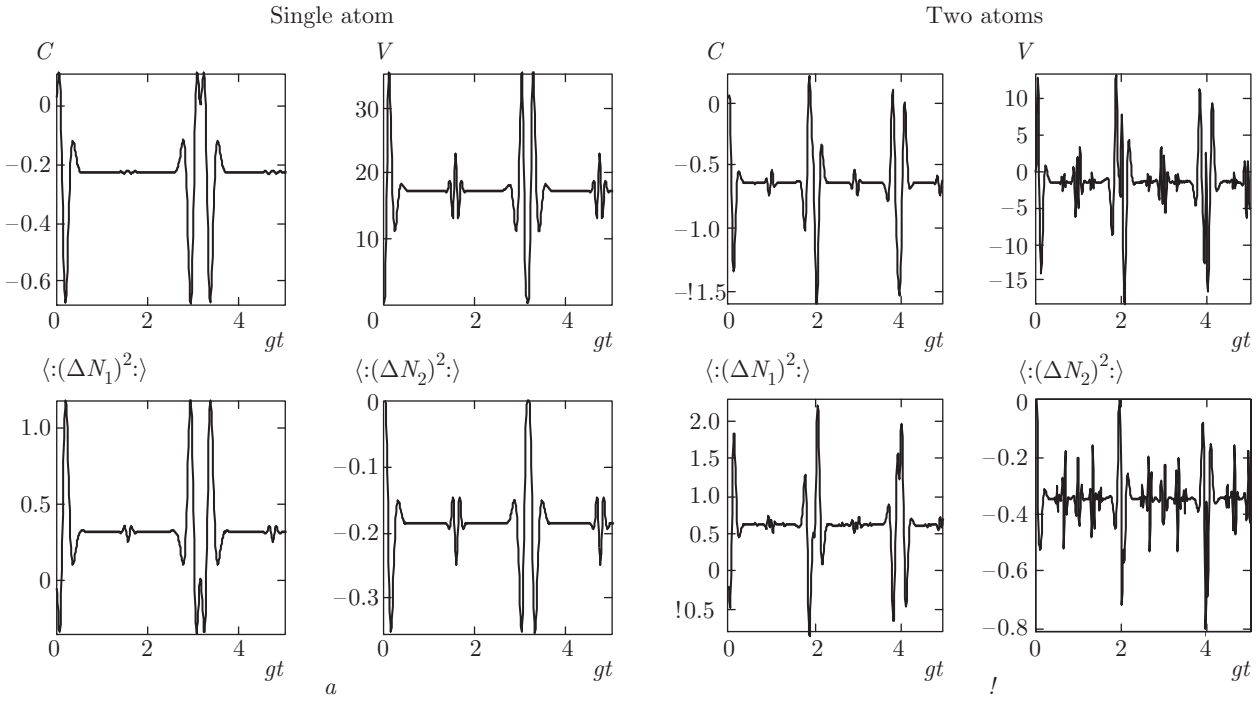

Fig. 4. Plots of $C(t)$, $V(t)$, $\langle :(\Delta N_1(t))^2:\rangle$, and $\langle :(\Delta N_2(t))^2:\rangle$ vs. gt for *a*) 1 atom and *b*) 2 atoms with $\overline{n}_1 = 10$, and $\overline{n}_2 = 0$

$$\langle a_1^\dagger(t)a_2^\dagger(t)a_2(t)a_1(t)\rangle_{SA} =$$

$$= \sum_{n_1=0}^{\infty}\sum_{n_2=0}^{\infty} n_1 n_2 P_{n_1}(\overline{n}_1)P_{n_2}(\overline{n}_2)|b_{n_1,n_2}|^2 +$$

$$+ \sum_{n_1=0}^{\infty}\sum_{n_2=0}^{\infty}(n_1-1)(n_2+1)P_{n_1}(\overline{n}_1)P_{n_2}(\overline{n}_2)\times$$

$$\times |a_{n_1-1,n_2+1}|^2. \quad (49)$$

We also consider the Cauchy–Schwartz inequality

$$\left(G_{12}^{(2)}(t)\right)^2 \le G_{11}^{(2)}(t)G_{22}^{(2)}(t), \quad (50)$$

which is violated by nonclassical states. We define the quantity [17, 19]

$$V(t) = \langle a_1^\dagger(t)a_2^\dagger(t)a_2(t)a_1(t)\rangle^2 -$$

$$- \langle a_1^{\dagger 2}(t)a_1^2(t)\rangle\langle a_2^{\dagger 2}(t)a_2^2(t)\rangle. \quad (51)$$

The Cauchy–Schwartz inequality is violated whenever $V(t) > 0$, indicating a nonclassical correlation between the two modes.

In Figs. 4*a* and 4*b*, we plot the time dependence of $C(t)$, $V(t)$, $\langle :(\Delta N_1(t))^2:\rangle$ and $\langle :(\Delta N_2(t))^2:\rangle$ for the respective single-atom and two-atom intensity-dependent Raman models in the case where the pump radiation mode is prepared initially in a coherent state whereas the Stokes radiation is in the vacuum state with $\overline{n}_1 = 10$ and $\overline{n}_2 = 0$. We observe the same strict periodicity in the collapse and revival as in the case of atomic probabilities.

From the numerical calculation of the cross-correlation function $C(t)$, we find that it is always negative (for both single atoms and two atoms) except at short time intervals. At the corresponding short time intervals, the beams become correlated. This is just in contrast to what happens in the two-mode ladder scheme with intensity-dependent coupling [13], where pairs of photons are emitted and absorbed together and the beams are always correlated except at short time regular intervals where they become anti-correlated (compare with Figs. 6 and 7 in Ref. [13]). Comparing Figs. 4*a* and 4*b*, we observe that the cross-correlation function $C(t)$ becomes more negative in the two-atom cases than in the case of a single atom. We thus obtain evidence of cooperative behavior in the production of anti-correlated beams. From the nature of the interaction where a photon from mode 1 is annihilated whereas another photon is created in mode 2, we expect the resulting modes to be predominantly anti-correlated, and this is to be summed up in the two-atom case.

In the single-atom case, we note in Fig. 4*a* that the Cauchy–Schwartz inequality is always violated since $V(t)$ is always positive, indicating a nonclassical correlation between the two modes. In the two-atom case, we observe in Fig. 4*b* that $V(t)$ is always negative except at a very short time interval in the transient regime and later at short time regular interval of the time $gt = 0.99,\ 1.99,\ 2.98,\ 3.98$, etc. A comparison of $V(t)$ for a single atom and for two atoms reveals that the Cauchy–Schwartz inequality is less strongly violated in the two-atom case than in the case of a single atom.

We note in Figs. 4*a* and 4*b* that mode 1 shows anti-bunching only at short time regular intervals for both single-atom and two-atom intensity-dependent Raman coupled models. At the corresponding short time intervals, the variances $\langle : (\Delta N_1(t))^2 : \rangle$ do become more negative for two atoms than the one-atom case. This is an indication of cooperative effects in producing anti-bunching in mode 1 at short time regular intervals.

It is observed that the normally ordered variance $\langle : (\Delta N_2(t))^2 : \rangle$ is always negative both for a single atom (Fig. 4*a*) and for two atoms (Fig. 4*b*), showing that a sub-Poisson statistics is always present in the second mode. It is observed that $\langle : (\Delta N_2(t))^2 : \rangle$ becomes more negative in the case of two atoms than in the case of a single atom.

5.1. Cooperative nonclassical effects

In our previous work on the ladder configuration with two atoms interacting with the intensity-dependent two-mode field, we found cooperative behavior in the production of correlated photons (Ref. [13], Fig. 6 (two atoms), Fig. 7 (single atom)). Here, for the intensity-dependent Raman coupled model, we also obtain evidence of cooperative behavior, but in the production of anti-correlated beams ($C < 0$).

Additionally in this paper, we also observe evidence for cooperative behavior in the production of photon anti-bunching (variance < 0) both in mode 1 (at short time intervals) and in mode 2 when a single input of photons is present. It is important to mention that the evidence for cooperative behavior in the production of antibunching was not observed in Ref. [13] for the intensity-dependent ladder scheme either in mode 1 (Ref. [13], Figs. 4*a*–5*a*) or in mode 2 (Ref. [13], Figs. 4*b*–5*b*) with a single input ($\overline{n}_1 = 8$, $\overline{n}_2 = 0$). These are important distinctions between the ladder and Raman schemes; we see how the schemes affect the cooperative behavior in production of nonclassical effects when single input photons are present.

Figures 5*a* and 5*b* show the time dependence of $C(t)$, $V(t)$, $\langle : (\Delta N_1(t))^2 : \rangle$, and $\langle : (\Delta N_2(t))^2 : \rangle$ for $\overline{n}_1 = 1$ and $\overline{n}_2 = 1$, keeping $\Delta = 0$ for a single atom and for two atoms respectively.

The effects of detuning on the evolution of $C(t)$, $V(t)$, $\langle : (\Delta N_1(t))^2 : \rangle$, and $\langle : (\Delta N_2(t))^2 : \rangle$ can be seen in Fig. 6 for large detuning ($\Delta = 20g$) with the same initial conditions as in Fig. 5 ($\overline{n}_1 = 1$ and $\overline{n}_2 = 1$) for a single atom and for two atoms.

We note that the oscillations become more rapid for large detuning. For two atoms, the oscillations are twice more rapid with the presence of two oscillation modes or suboscillations.

6. CONCLUSIONS

We have discussed the dynamics for the collective two-atom Raman coupled model interacting with a quantized bimodal field with intensity-dependent coupling terms. The dynamics of the atomic level populations have been studied and expressions for the collapse time and the revival time have been obtained.

We examined some aspects of photon statistics and compared the results with the two-mode ladder model with intensity-dependent coupling in Ref. [13]. We note that just like in the ladder scheme with intensity-dependent coupling (Ref. [13]), where cooperative behavior in the production of correlations in the light beam is observed, in the intensity-dependent Raman coupled model, we also obtain evidence of cooperative behavior in the production of anti-correlated beams, although the correlations between the two modes do not become more nonclassical. Additionally in this paper, we also observe evidence for cooperative behavior in the production of anti-bunching in both modes with a single input photon present. Here, it is important to note that the evidence of cooperative behavior in producing the antibunching is not observed in the ladder scheme (Ref. [13]) either in mode 1 or in mode 2 when a single input photon is present.

It is also observed that with an increase in detuning, the oscillations become more rapid. For two atoms, the oscillations are twice more rapid due to suboscillations in the Raman scheme.

Although our study is limited to short-time behavior, we obtained analytic expressions that are convenient and provide some useful insights into the dynamics. Our focus here is on the effects of the Raman scheme with intensity dependence. The effects of dissipation at long times will be deferred for future investigations.

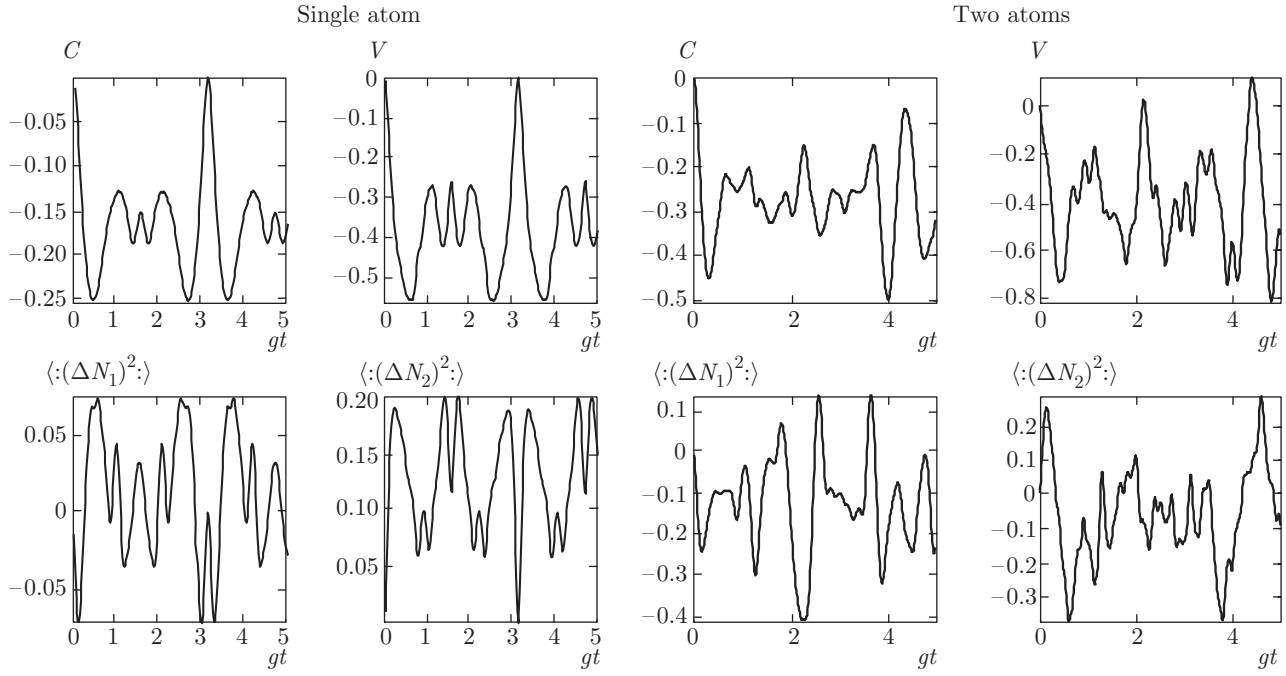

Fig. 5. Plots of $C(t)$, $V(t)$, $\langle: (\Delta N_1(t))^2 :\rangle$, and $\langle: (\Delta N_2(t))^2 :\rangle$ vs. gt for 1 atom and 2 atoms with $\overline{n}_1 = 1$ and $\overline{n}_2 = 1$ for zero detuning

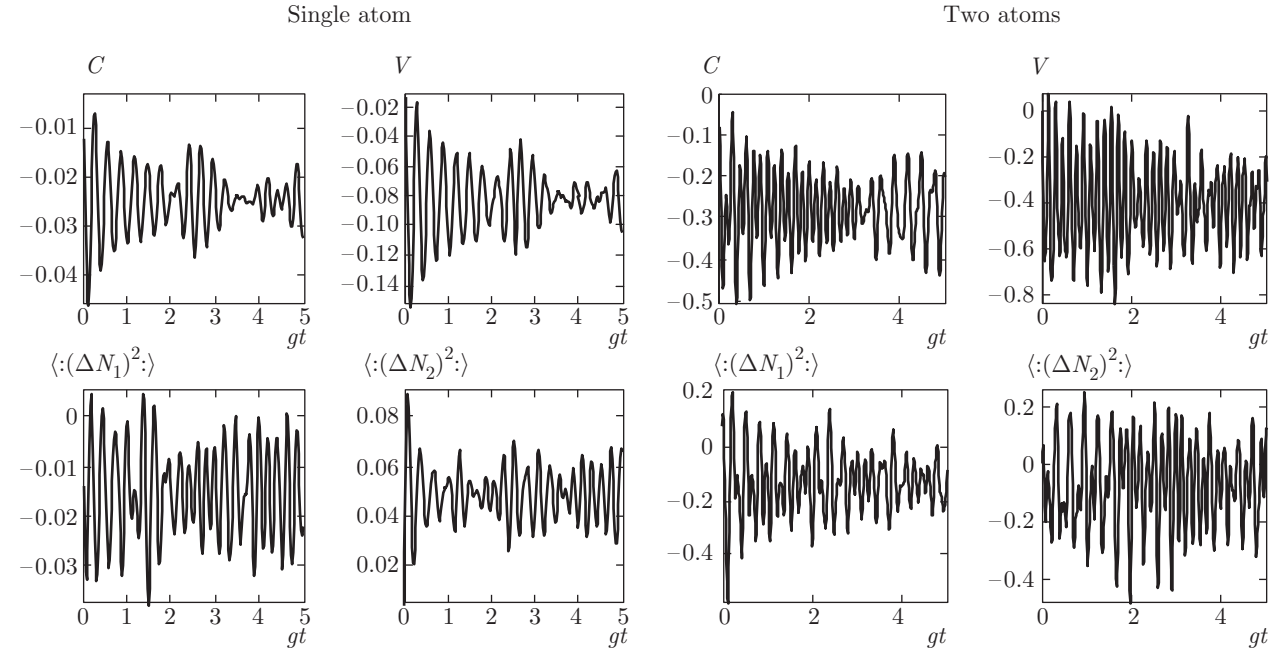

Fig. 6. Plots of $C(t)$, $V(t)$, $\langle: (\Delta N_1(t))^2 :\rangle$, and $\langle: (\Delta N_2(t))^2 :\rangle$ vs. gt for 1 atom and 2 atoms with $\overline{n}_1 = 1$ and $\overline{n}_2 = 1$ for the large detuning $\Delta = 20g$

APPENDIX

The expression for the general state vector is obtained as

$$
\begin{aligned}
|\psi(t)\rangle = [1 - it(\omega_1 n_1 + \omega_2 n_2 - \omega_0) - \\
- \frac{t^2}{2!}\left\{(\omega_1 n_1 + \omega_2 n_2 - \omega_0)^2 + 2g^2 n_1^2 (n_2+1)^2\right\} + \\
+ \frac{it^3}{3!}\left\{(\omega_1 n_1 + \omega_2 n_2 - \omega_0)^3 + 2g^2 n_1^2 (n_2+1)^2 \times\right. \\
\times [2\omega_1 n_1 + 2\omega_2 n_2 - 2\omega_0 + \omega_1(n_1-1) + \omega_2(n_2+1)]\} + \\
+ \frac{t^4}{4!}\left\{(\omega_1 n_1 + \omega_2 n_2 - \omega_0)^4 + 2g^2 n_1^2 (n_2+1)^2 \times\right. \\
\times \left[3\omega_0^2 - 6\omega_0\omega_1 n_1 - 2\omega_0\omega_1(n_1-1) + 3\omega_1^2 n_1^2 - \right. \\
- 2\omega_0\omega_2(n_2+1) + 2\omega_1^2(n_1-1)n_1 + 6\omega_1 n_1 \omega_2 n_2 + \\
+ 2\omega_1 n_1 \omega_2(n_2+1) + 2\omega_1(n_1-1)\omega_2 n_2 + \\
+ 3\omega_2^2 n_2^2 + 2\omega_2^2 n_2(n_2+1) + 2g^2 n_1^2 (n_2+1)^2 - \\
- 6\omega_0\omega_2 n_2 + 2g^2(n_1-1)^2(n_2+2)^2 + \omega_1^2(n_1-2)^2 + \\
\left. + \omega_2^2(n_2+1)^2 + 2\omega_1(n_1-1)\omega_2(n_2+1)\right]\} + \ldots] \times \\
\times |0, n_1, n_2\rangle + \left[-it 2g n_1(n_2+1) - \frac{t^2}{2!} 2g n_1(n_2+1) \times\right. \\
\times \{\omega_1 n_1 - \omega_0 + \omega_1(n_1-1) + \omega_2(n_2+1) + \omega_2 n_2\} + \\
+ \frac{it^3}{3!} 2g n_1(n_2+1)\left\{(2g^2 n_1^2 (n_2+1)^2 + 2g^2(n_1-1)^2(n_2+2)^2 + \right. \\
+ \omega_0^2 + \omega_1^2(n_1-1)^2 + \omega_1^2 n_1(n_1-1) + \omega_1^2 n_1^2 + \omega_2^2(n_2+1)^2 + \\
+ \omega_2^2(n_2+1)(n_2+2) + \omega_2^2 n_2(n_2+1) - \\
- 2\omega_0\omega_2 n_2 - \omega_0\omega_2(n_2+1) - \\
- \omega_0\omega_1(n_1-1) - 2\omega_0\omega_1 n_1 + \omega_2^2 n_2^2 + 2\omega_1(n_1-1) \times \\
\times \omega_2(n_2+1) + \omega_1 n_1 \omega_2(n_2+1) + \\
\left. + 2\omega_1 n_1 \omega_2 n_2 + \omega_1(n_1-1)\omega_2 n_2)\} + \ldots\right] \times \\
\times |1, n_1-1, n_2+1\rangle + \left[-\frac{t^2}{2!} 2g^2 n_1(n_1-1)(n_2+1)(n_2+2) + \right. \\
+ \frac{it^3}{3!} 2g^2 n_1(n_1-1)(n_2+1)(n_2+2)\{\omega_1(n_1-2) + \omega_1(n_1-1) + \\
+ \omega_1 n_1 + \omega_2(n_2+2) + \omega_2(n_2+1) + \omega_2 n_2\} + \\
+ \frac{t^4}{4!} 2g^2(n_1-1)n_1(n_2+1)(n_2+2)\left\{2g^2 n_1^2(n_2+1)^2 + \right. \\
+ 2g^2(n_1-1)^2(n_2+2)^2 + \omega_0^2 + \omega_2^2(n_2+2)^2 + \omega_2^2 n_2^2 + \\
+ \omega_2^2 n_2(n_2+2) + \omega_2^2(n_2+1)^2 + \omega_2^2(n_2+1)(n_2+2) + \\
+ \omega_2^2 n_2(n_2+1) + \omega_1^2(n_1-2)^2 + \omega_1^2 n_1^2 + \omega_1^2(n_1-2)n_1 + \\
+ \omega_1^2(n_1-1)^2 + \omega_1^2(n_1-2)(n_1-1) + \omega_1^2(n_1-1)n_1 + \\
+ \omega_0\omega_1(n_1-2) - \omega_0\omega_1 n_1 - \omega_0\omega_2 n_2 + \omega_0\omega_2(n_2+2) + \\
+ 2\omega_1 n_1 \omega_2 n_2 + 2\omega_1(n_1-2)\omega_2(n_2+2) + \\
+ \omega_1 n_1 \omega_2(n_2+2) + \omega_1(n_1-2)\omega_2 n_2 + \omega_1 n_1 \omega_2(n_2+1) + \\
+ \omega_1(n_1-1)\omega_2 n_2 + \omega_1(n_1-2)\omega_2(n_2+1) + \omega_1(n_1-1) \times \\
\left.\left. \times \omega_2(n_2+2) + 2\omega_1(n_1-1)\omega_2(n_2+1)\right\} + \ldots\right] \times \\
\times |2, n_1-2, n_2+2\rangle.
\end{aligned}
$$

REFERENCES

1. E. T. Jaynes and F. W. Cummings, Proc. IEEE **51**, 89 (1963).
2. B. Buck and C. V. Sukumar, Phys. Lett. A **81**, 132 (1981).
3. C. V. Sukumar and B. Buck, Phys. Lett. A **83**, 211 (1981).
4. P. Zhou, Z. L. Hu, and J. S. Ping, J. Mod. Opt. **39**, 49 (1992).
5. V. Buzek, J. Mod. Opt. **36**, 1151 (1989).
6. P. Zhou, J. S. Ping, and G. X. Li, Acta Opt. Sin. **13**, 444 (1993).
7. Sudha Singh and Amrita, Int. J. Theor. Phys. **51**, 838 (2012).
8. Sudha Singh and Ashalata Sinha, Pramana–Journal of Phys. **70**, 887 (2008).
9. A. Napoli and A. Messina, J. Mod. Opt. **43**, 649 (1996).
10. X. Yang, Y. Wu, and Y. Li, Phys. Rev. A **55**, 4545 (1997).
11. C. Huang, L. Tang, F. Kong, J. Fang, and M. Zhou, Physica A **368**, 25 (2006).
12. Y.-F. Gao, J. Feng, and S.-R. Shi, Int. J. Theor. Phys. **41**, 867 (2002).
13. Sudha Singh, C. H. Raymond Ooi, and Amrita, Phys. Rev. A **86**, 023810 (2012).
14. R. H. Dicke, Phys. Rev. **93**, 99 (1954).
15. M. Butler and P. D. Drummond, Opt. Acta **33**, 1 (1986).
16. C. C. Gerry and J. B. Togeas, Opt. Commun. **69**, 263 (1989).
17. C. C. Gerry and H. Huang, Phys. Rev. A **45**, 8037 (1991).
18. D. A. Cardimona, V. Kovanis, M. P. Sharma, and A. Gavrielides, Phys. Rev. A **43**, 3710 (1991).
19. C. C. Gerry and J. H. Eberly, Phys. Rev. A **42**, 6805 (1990).
20. M. Alexamian and S. K. Bose, Phys. Rev. A **52**, 2218 (1995).
21. S. Singh, Phys. Rev. A **25**, 3206 (1982).
22. Sudha Singh, Pramana–Journal of Phys. **66**, 615 (2006).
23. Y. Wu, Phys. Rev. A **54**, 1586 (1996).
24. R. Loudon, Rep. Prog. Phys. **43**, 58 (1980).